HEAT GENERATION AND ABSORPTION IN MHD FLOW OF CASSON FLUID PAST A STRETCHING WEDGE WITH VISCOUS DISSIPATION AND NEWTONIAN HEATING

Imran Ullah[a], Sharidan Shafie[a], Ilyas Khan[b]

[a]Department of Mathematical Sciences, Faculty of Science, Universiti Teknologi Malaysia, 81310 UTM Johor Bahru, Johor, Malaysia
[b]Majmaah University, Majmaah, Saudi Arabia

Graphical abstract
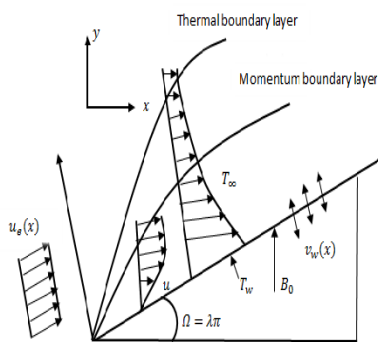
Abstract

The dissipative flow of Casson fluid in the presence of heat generation and absorption is investigated. The flow is induced due to stretching wedge. The similarity transformations were used to to transformed the governing equations into ordinary differential equations. The transformed equations are solved numerically via Keller-box method. Numerical results for skin friction coefficient are compared and found in excellent agreement with published results. The effects of pertinent parameters on velocity and temperature profiles as well as skin friction and heat transfer rate are graphically displayed and analyzed. It is noticed that fluid velocity drops with the increase of Casson fluid and magnetic parameters when the wedge is stretching faster than free stream. It is also noted that the heat transfer rate at wedge surface reduces with the increase of Eckert number, whereas the reverse trend is noted in the case of Casson and radiation parameters. Moreover, with increasing of heat generation or absorption parameter the fluid temperature rises.

Keywords: Casson fluid, stretching wedge, MHD, heat generation, viscous dissipation

1.0 INTRODUCTION

In the last few decades, the study of non-Newtonian fluids has gained considerable attention because of its wide range applications in engineering and industry. Due to the complex nature of these fluids, no single constitutive equation is available to possess all properties of such fluids. Various models have been suggested in this regard. In literature, power law model is mostly used for non-Newtonian fluids. The reason is that mathematically, these fluids are easy to tackle among other non-Newtonian fluids. Casson fluid model is also one of the non-Newtonian model. Casson model was first used by Casson [1] for preparation of printing inks and silicon suspensions. It is thought to be the more suitable for rheological data by many researchers.

Furthermore, it is preferred rheological model for blood and chocolate. Casson fluid exhibits yield stress. The fluid behaves like solid if the applied shear stress is less than yield stress, whereas for greater shear stress, it starts moving [2, 3].

Falkner and Skan [4] for the first time employed similarity transformation and solved wedge problem numerically. Later on, several researchers have extended this problem for different types of fluids and considered the wedge as static, moving or stretching inside the fluid. Ishak *et al.* [5] studied the two dimensional flow of viscous fluid past a moving wedge. Yacob *et al.* [6] investigated the laminar flow over a

static or a moving wedge saturated in nanofluid numerically. Postelnicu and Pop [7] analyzed boundary layer flow of power law fluid past a permeable stretching wedge using similarity transformations. Mukhopadhyay *et al.* [8] and Mukhopadhyay and Mandal [9] studied numerically the forced convection flow of Casson fluid past a symmetric non-porous and porous wedge, respectively. They found that shear stress is decreasing function of the Casson fluid parameter.

In the recent years, the study of magnetohydrodynamic (MHD) boundary layer has been the attention of several researchers due to its wide range applications in engineering and technology. For instance, MHD pumps, MHD power generators, design for cooling of nuclear reactors, flow meters, blood flow measurement, and construction of heat exchangers and in many other systems using electrically conducting fluids. Yih [10] and Chamkha *et al.* [11] explored numerically MHD forced convection flow of viscous fluid adjacent to non-isothermal wedge. MHD mixed convection flow of viscous fluid past a permeable stretching wedge is presented by Su *et al.* [12]. Prasad *et al.* [13] studied the magnetic effects on the boundary layer flow of viscous fluid past a non-isothermal permeable wedge. They concluded that magnetic parameter and suction reduces the thermal boundary layer thickness. El-Dabe *et al.* [14] studied two dimensional heat and mass transfer flow of Casson fluid due to a moving wedge under the influence of magnetic field. Recently, Hsiao [15] investigated electrically conducting flow of Viscoelastic Carreau fluid in the presence of nanoparticles.

The phenomenon of heat generation or absorption in working fluid plays a vital role in several engineering and industries. The impact of heat generation may boost the temperature distribution in moving fluids, and consequently, influences he heat transfer rate. Its application can be found in several industries, for instance, removal of heat from nuclear debris, food storage, geothermal system, cooling of nuclear reactors, thermal absorption and microelectronics manufacturing. Salem and El-Aziz [16] investigated the effects of heat generation and absorption in electrically conducting flow of viscous fluid in the presence of chemical reaction. They concluded that heat generation and absorption has a significant effect on temperature field. The influence of heat generation or absorption on two dimensional flow of micropolar fluid generated due to stretching sheet has been analyzed by Magyari nd Chamkha [17].

Later on, Ahmad and Khan [18] examined the combined effects of viscous dissipation and heat generation or absorption on convective flow of viscous fluid past a moving wedge. They found the similarity solutions using fourth order Runge-Kutta scheme along with shooting method. They noticed that temperature distribution is more influenced with increase in Eckert number. Nandy and Mahapatra [19] studied numerically the effects of heat generation and absorption on MHD flow of nanofluid in the presence

of slip and convective boundary conditions. The variation of heat generation on mixed convection flow of nanofluid over a stretching sheet embedded in a porous medium was reported by Pal and Mandal [20]. The influence of heat generation and absorption on stagnation point flow in the presence of nanoparticles was analyzed by Hsiao [21].The combined effects of MHD and heat generation/absorption on heat transfer flow of Maxwell fluid in the presence of viscous dissipation was reported by Hsiao [22] Very recently, the similarity solutions on mixed convection flow over a horizontal surface through porous medium were provided by Ferdows and Liu [23].

From the existing literature, it is evident that the effects of heat generation and absorption on Casson fluid over a wedge is not been investigated. Also, very less attention is paid towards the stretching wedge, although stretching surfaces have important applications in manufacturing processes of plastic and metal industries. To the best of authors' knowledge, no attempt is made so far to study hydromagnetic forced convection flow of Casson fluid over a porous stretching wedge. The objective of present analysis is to study the effects of heat generation or absorption and viscous dissipation on electrically conducting flow of Casson fluid due to stretching wedge in the presence of Newtonian heating. The non-linear governing equations are transformed into non-linear ordinary differential equations using similarity transformations and then solved numerically by Keller-box method [24].

2.0 METHODOLOGY

Consider the steady two dimensional incompressible flow of Casson fluid induced by permeable stretching wedge in the presence of applied magnetic field $B(x) = B_0 x^{\frac{m-1}{2}}$ with B_0 is the strength of magnetic field. The magnetic Reynolds number is small enough such that the induced magnetic field is neglected. It is assumed that wedge stretches with velocity of $u_w(x) = \gamma u_e(x)$, $\gamma \geq 0$ and the free stream velocity $u_e(x) = U_\infty x^m$, where $0 \leq m \leq 1$ and U_∞ are constants (see Figure 1). $\lambda = \frac{2m}{m+1}$ is the wedge angle parameter that corresponds to $\Omega = \lambda\pi$ for the total angle of the wedge.
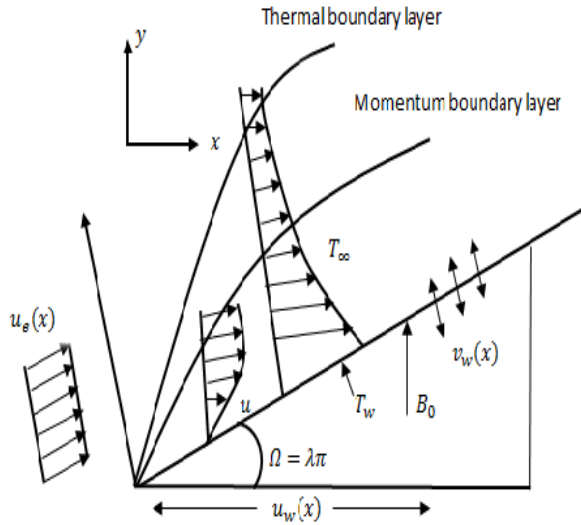
Figure 1 Physical coordinate system of the problem

The governing equations of continuity, momentum and energy are written as

$$\frac{\partial u}{\partial x} + \frac{\partial u}{\partial y} = 0 \qquad (1)$$

$$u\frac{\partial u}{\partial x} + v\frac{\partial u}{\partial y} = u_e\frac{\partial u_e}{\partial x} + v\left(1 + \frac{1}{\beta}\right)\frac{\partial^2 u}{\partial y^2} + \frac{\sigma B^2(x)}{\rho}(u_e - u) \qquad (2)$$

$$u\frac{\partial T}{\partial x} + v\frac{\partial T}{\partial y} = \frac{k}{\rho c_p}\frac{\partial^2 T}{\partial y^2} - \frac{1}{\rho c_p}\frac{\partial q_r}{\partial y} + \frac{v}{c_p}\left(1 + \frac{1}{\beta}\right)\left(\frac{\partial u}{\partial y}\right)^2$$

$$+ \frac{\sigma B^2(x)}{\rho c_p}(u_e - u)^2 + v\frac{Q(x)}{\rho c_p}(T - T_\infty) \qquad (3)$$

where u and v denote the velocity components in x and y directions respectively, v is kinematic viscosity, σ is the electrically conductivity, ρ is the fluid density, β is the Casson parameter, T is the fluid temperature, T_∞ is the temperature at free stream, k is the thermal conductivity of the fluid, c_p is the specific heat at constant pressure, $q_r = -\frac{4\sigma^*}{3k_1^*}\frac{\partial T^4}{\partial y}$ is the Rosseland approximation, σ^* is the Stefan-Boltzman constant, k_1 is the mean absorption coefficient and $Q(x) = Q_0 x^{m-1}$ is the heat generation or absorption coefficient.

The corresponding boundary conditions are written as follows:

$$u = u_w(x) = \gamma u_e(x), v = v_w(x), \frac{\partial T}{\partial y} = -h_s T \text{ at } y = 0 \qquad (4)$$

$$u = u_e(x), T \to T_\infty \text{ as } y \to \infty \qquad (5)$$

where $v_w(x) = V_0\sqrt{x^{m-1}}$ is the velocity at the wall with constant V_0. Here $v_w(x) > 0$ is the injection velocity and $v_w(x) < 0$ is the suction velocity, respectively. The constant parameter $\gamma = \frac{U_w}{U_\infty}$ is velocity ratio parameter

of wedge such that $\gamma > 1$ corresponds to faster stretching of wedge than that of free stream and $\gamma < 1$ corresponds to slower than that of free stream flow and $h_s(x) = h_0 x^{\frac{m-1}{2}}$ is the convective heating transfer. Now introducing the following similarity transformations

$$\Psi = \sqrt{\frac{2vxu_e}{m+1}}f(\eta), \eta = \sqrt{\frac{(m+1)u_e}{2vx}}y, \theta = \frac{T - T_\infty}{T_\infty} \qquad (6)$$

where the stream function Ψ is defined by the following relations:

$$u = \frac{\partial \Psi}{\partial y}, v = -\frac{\partial \Psi}{\partial x} \qquad (7)$$

From equations $(2) - (5)$, one arrives at the following non-dimensional system

$$\left(1 + \frac{1}{\beta}\right)f''' + ff'' + \lambda(1 - f'^2) + (2 - \lambda)M(1 - f') = 0 \qquad (8)$$

$$\frac{1}{Pr}(1 + N)\theta'' + f\theta' + \left(1 + \frac{1}{\beta}\right)Ecf''^2$$

$$+ (2 - \lambda)MEc(1 - f')^2 + (2 - \lambda)\varepsilon\theta = 0 \qquad (9)$$

$$f(0) = \sqrt{(2 - \lambda)}S, f'(0) = \gamma,$$

$$\theta'(0) = -\sqrt{(2 - \lambda)}\delta[1 + \theta(0)] \qquad (10)$$

$$f'(\infty) = 1, \theta(\infty) = 0 \qquad (11)$$

where $M = \frac{\sigma B_0^2}{\rho U_\infty}$ is the magnetic field parameter, $Pr = \frac{\mu c_p}{k}$ is the Prandtl number, $N = \frac{16\sigma^* T_\infty^3}{3kk_1^*}$ is the radiation parameter, $Ec = \frac{u_e^2}{c_p T_\infty}$ is the Eckert number, $\varepsilon = \frac{Q_0}{c_p U_\infty}$ is the heat generation and absorption parameters, $\delta = h_0\left(\frac{2v}{U_\infty}\right)^{1/2}$ is the Newtonian heating parameter and $S = \frac{-V_0}{\sqrt{U_\infty v}}$ is the suction/injection parameter such that $S(>0)$ is suction velocity $S(<0)$ is injection velocity and $S(=0)$ represents impermeable wedge.

The parameters with physical interests are the skin friction coefficient Cf_x and local Nusselt number Nu_x which are defined as follows:

$$Cf_x(Re_x)^{1/2} = \frac{\tau_w}{\rho u_e^2} = \sqrt{\frac{1}{(2-\lambda)}}\left(1 + \frac{1}{\beta}\right)f''(0)$$

$$Nu_x(Re_x)^{-1/2} = \frac{xq_w}{k(T_w - T_\infty)} = -\sqrt{\frac{1}{(2-\lambda)}}\theta'(0)$$
$$\qquad (12)$$

where τ_w is the wall skin friction, q_w is the wall heat flux and $Re_x = \frac{xu_e}{v}$ is the local Reynold number.

Table 1 Comparison of the skin friction coefficient $f''(0)$ with various values of S for $M = \gamma = 0$, $\lambda = 1$ and $\beta \to \infty$.

			$f''(0)$		
S	Yih [10]	Ahmad and Khan [18]	Ishak *et al.* [5]	Postelnicu and Pop [7]	Present results
-1	0.75658	0.75655	0.7566	0.75657	0.7566
-0.5	0.96923	0.96922	0.9692	0.96923	0.9692
0	1.23259	1.23258	1.2326	1.23259	1.2326
0.5	1.54175	1.54175	1.5418	1.54175	1.5418
1	1.88931	1.88931	1.8893	1.88931	1.8893

3.0 RESULTS AND DISCUSSION

In order to analyze the results, numerical calculations are carried out for various values of Casson fluid parameter β, wedge angle parameter λ, magnetic parameter M, stretching wedge parameter γ, Prandtl number Pr, radiation parameter N, Eckert number Ec, heat generation or absorption parameter ε, suction/injection parameter S and Newtonian heating parameter δ. It need to be mentioned at this stage that the step size used in this study is $\Delta\eta = 0.001$. The boundary layer thickness $\eta_{max} = 10$ is taken. Moreover, the solution is assumed as converged when the difference between two consective values remained 10^{-5}. After obtaining a converged solution, the computation will continue by marching in the $\eta-$ direction.

In order to validate and check the accuracy of the Keller box method. The results for wall shear stress are compared with the results of Yih [10], Ahmad and Khan [18], Ishak *et al.* [5] and Postelnicu and Pop [7], and are shown in Table 1. Comparison reflected an excellent agreement among them.

Figures (2-4) are plotted to analyze the effects of β, M and S on velocity profile, respectively. It is noteworthy here that the present phenomenon reduces to viscous fluid as $\beta \to \infty$. From Figure 2, it is observed that fluid velocity is decreasing with increase of β when $\gamma > 1$ whereas fluid velocity enhances with β when $\gamma < 1$. In other words, the absolute values of shear stress increase with the increase of β and momentum boundary layer thickness reduces for $\gamma > 1$ or $\gamma < 1$. As it is obvious, that magnitude of velocity in Casson fluid is greater than viscous fluid. It is also noted that skin friction is zero when $\gamma = 1$ and velocity of fluid becomes uniform. Furthermore, the velocity has inverted boundary layer pattern for $\gamma < 1$. In this case, the velocity of stretching wedge is stipulated by velocity of free stream.
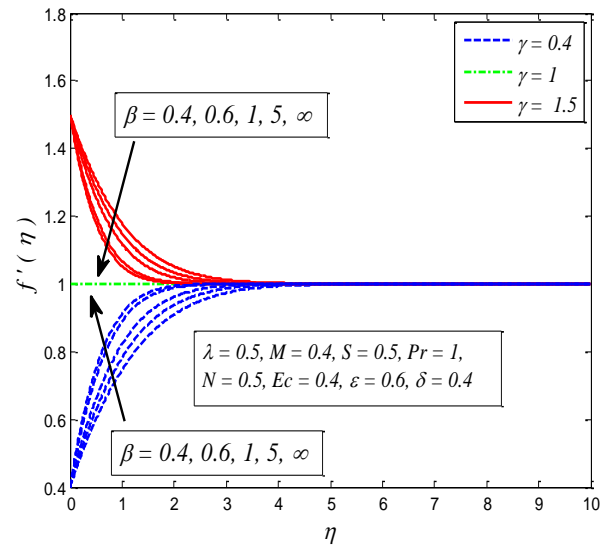
Figure 2 Effect of β on velocity for various γ

The variation of M on velocity profile is illustrated in Figure 3. It is observed that for $\gamma > 1$ the velocity of Casson fluid decreases as M increases whereas the velocity of fluid is strongly accelerated for $\gamma < 1$ when M increases. The explanation for this phenomenon is that application of transverse magnetic field in an electrically conducting fluid produces a drag force, known as Lorentz force. This force has the tendency to retard the fluid motion.

The effect of S on velocity profile is displayed in Figure 4. It is noticed that fluid velocity is reduced in case of suction and arises in the case of injection when $\gamma > 1$ whereas the case of $\gamma < 1$ is opposite to this phenomenon.
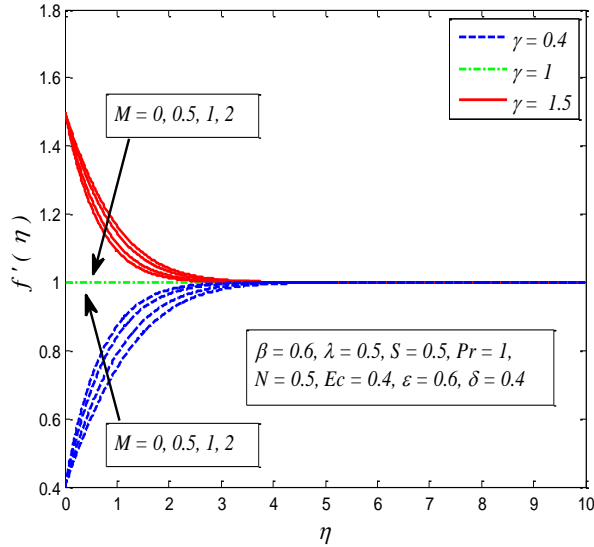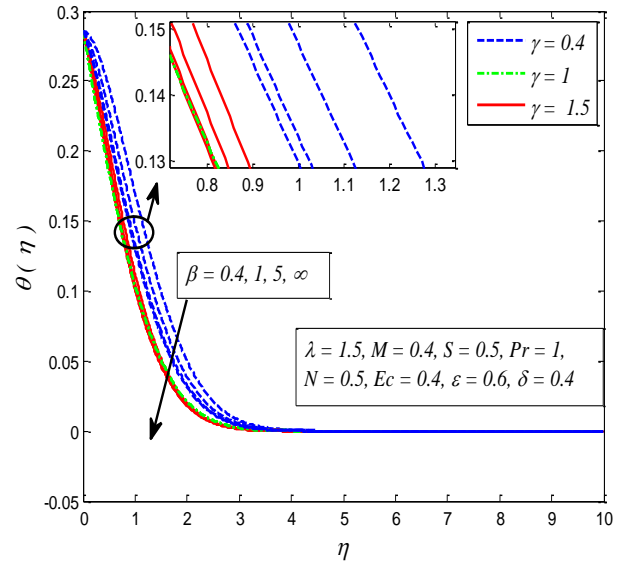
Figure 3 Effect of *M* on velocity for various *γ*

It is well known fact that when suction is applied to the wall, it shows resistance to the flow and resulting a decrease in momentum boundary layer thickness.
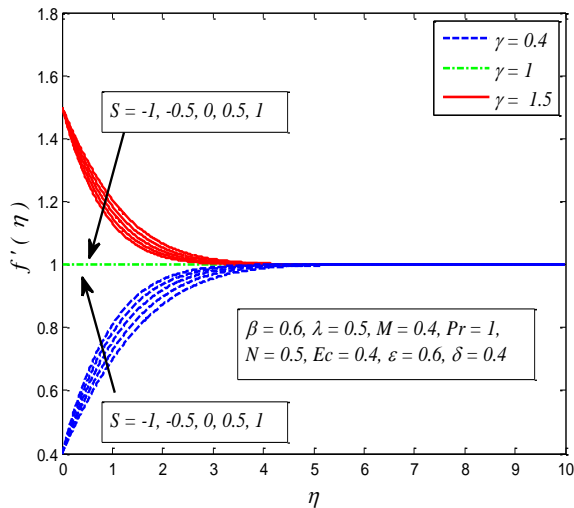

Figure 4 Effect of *S* on velocity for various *γ*

Figures (5-12) exhibit the effects of β, M, S, Pr, N, Ec, ε and δ on dimensionless temperature, respectively. Figure 5 demonstrates that fluid temperature decreases with increase of β for both $\gamma < 1$ and $\gamma > 1$.

Figure 5 Effect of β on temperature for various γ

Figure 6 clearly shows that temperature reduces as M increases when $\gamma < 1$ and $\gamma > 1$. Figure 7 illustrates that temperature decreases in the case of suction, whereas injection enhances the fluid temperature either $\gamma > 1$ or $\gamma < 1$. In fact, injection is often used for protection of surfaces as it reduces the rate of heat transfer.
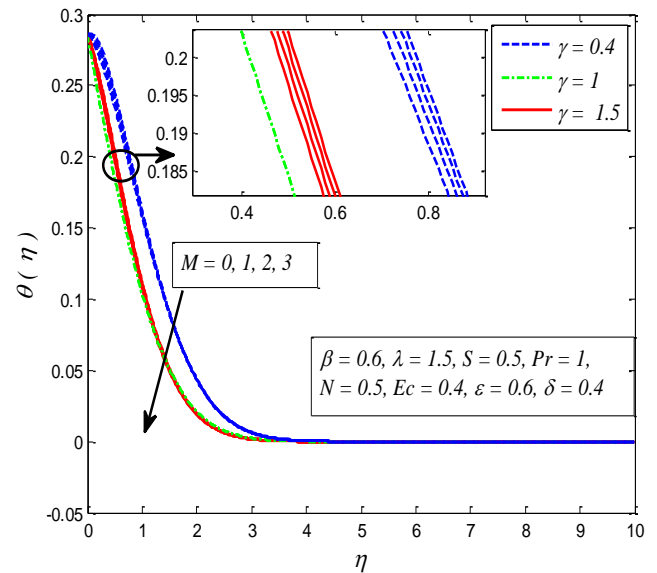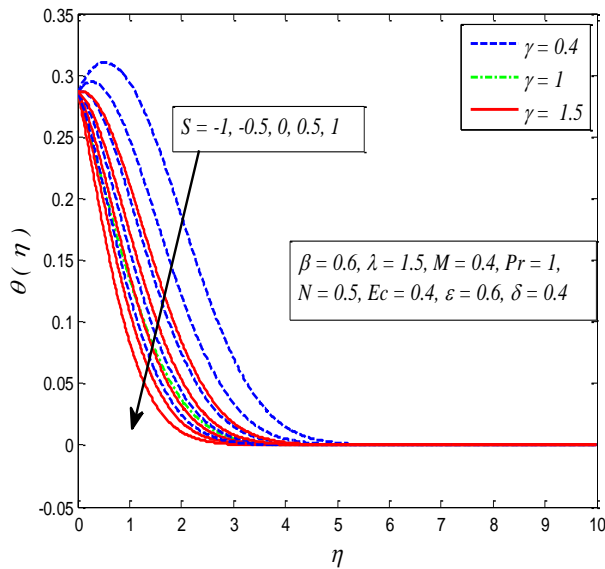

Figure 6 Effect of M on temperature for various γ

Figure 7 Effect of S on temperature for various γ

reduces to the case of prescribed wall temperature when $\delta \to \infty$. As δ depend upon the heat transfer coefficient, therefore larger values of δ lead to enhance the heat transfer rate.
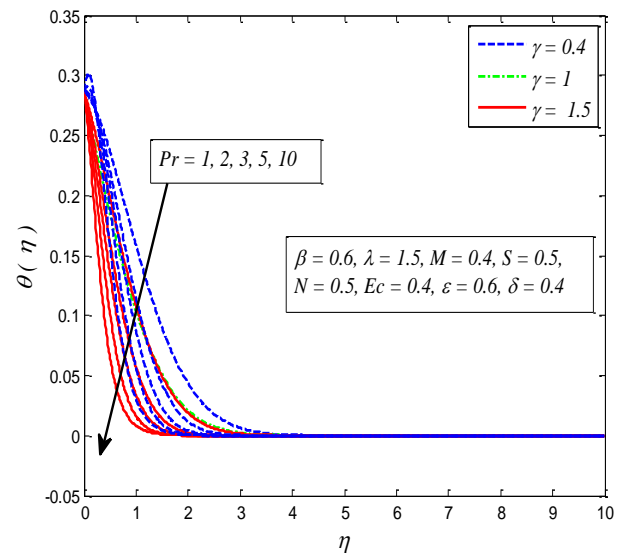

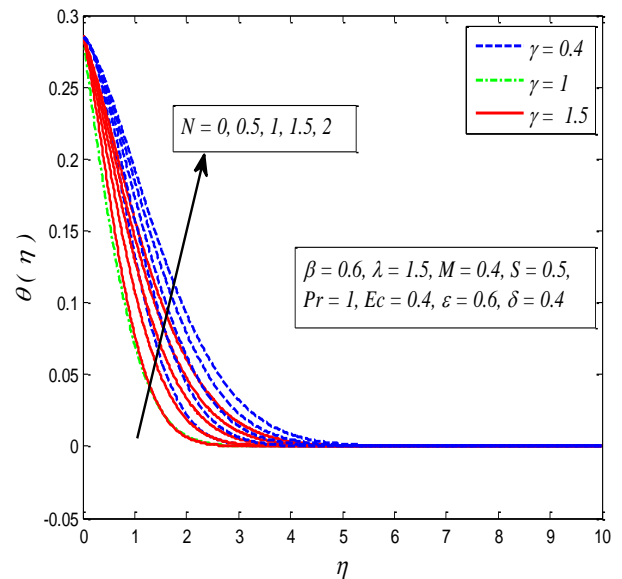**Figure 8** Effect of Pr on temperature for various γ

As expected, Figure 8 describes that the temperature as well as thermal boundary layer thickness decrease with increase of Pr. It is also observed that higher values of Pr reduces the temperature significantly and thermal boundary layers are squeezing closer and closer to the wall. As Prandtl number is defined as the ratio of momentum diffusivity to thermal diffusivity which means that increasing Pr tends to decrease the thermal diffusivity; and as a result temperature reduces. Hence, Prandtl number is useful in conducting flows to enhance the cooling rate. Figure 9 presents that temperature is higher for higher values of N. This behavior agrees with the fact that the increase in radiation produces the kinetic energy, due to which velocity get accelerated and as a consequences the thermal boundary layer becomes thicker. A similar behavior of temperature profile is noticed by the increase of Ec, as plotted in Figure 10. Since energy stores in the fluid as dissipative heat occurs. A peak near the wedge surface is also observed with higher values of Ec. The reason is that stronger dissipative force enhances the frictional heating between the wedge surface and fluid particles, thereby fluid temperature excites near the wall and thermal boundary layer becomes thicker. Figure 11 reveals the influence of ε on temeperature profile. It is necessary to mention here that $\varepsilon < 0$ describes heat absorption and $\varepsilon > 0$ corresponds to heat generation. It is observed that the temperature falls when $\varepsilon < 0$ whereas, it enhances when $\varepsilon > 0$ in both cases of $\gamma < 1$ and $\gamma > 1$. Since the existence of heat generation causes an increase in thermal energy of working fluid, thereby it raises the temperature. The case of absorption is opposite to this phenomenon. Figure 12 depicts that temperature and associated boundary layer thickness enhances with the growth of δ. It is worth to mention that the present problem

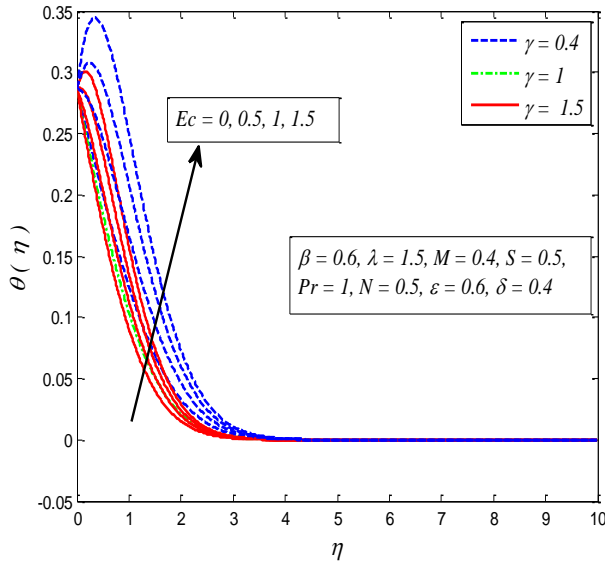**Figure 9** Effect of N on temperature for various γ

Figure 10 Effect of Ec on temperature for various γ

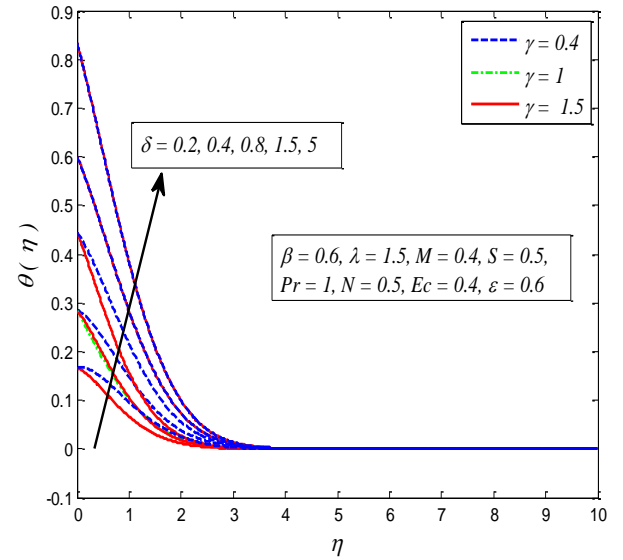**Figure 12** Effect of δ on temperature for various γ
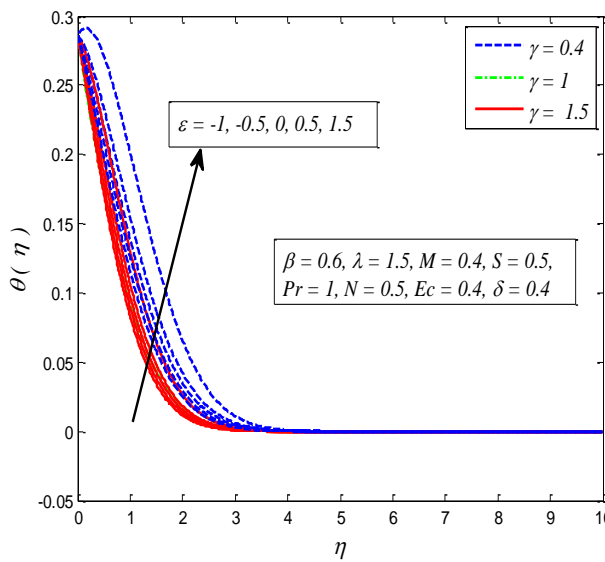

Figure 11 Effect of ε on temperature for various γ

Figures 13 and 14 portray the variation of skin friction coefficient and Nusselt number for different β, M, S, Ec and N respectively. From Figure 13 it is noticed that skin friction coefficient declines with the increase of β whereas, increasing values of M and S excite the friction factor.
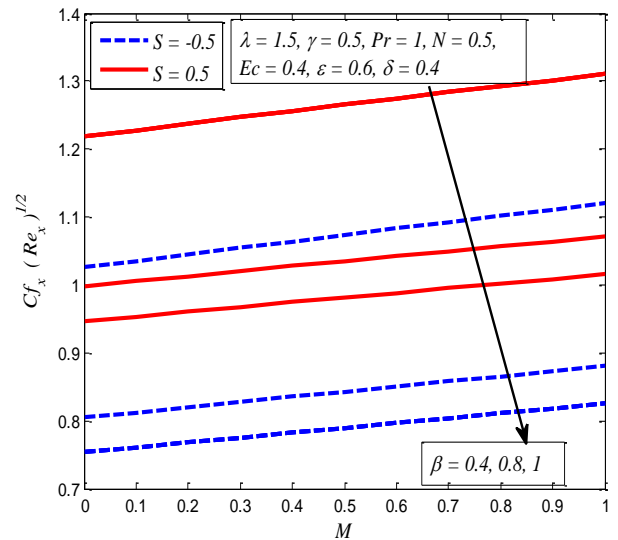

Figure 13 Variation of skin friction coefficient for various $\beta, M,$ and S

From Figure 14, it is seen that Nusselt number, which is also known as heat transfer rate is higher at the wedge surface with the increasing values of N and β whereas, opposite trend is noticed when Ec increased.
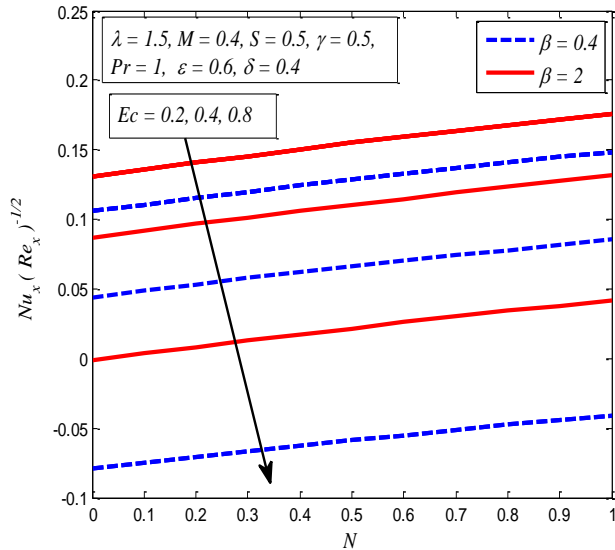
Figure 14 Variation of Nusselt number for various β, N and Ec

4.0 CONCLUSION

In this paper, the influence of heat generation and absorption on the electrically conducting flow of Casson fluid with characteristics of heat transfer over stretching wedge is studied. The similarity solutions are obtained by Keller-box method. The accuracy of method is checked through comparison with the results of available literature and revealed in close agreement. Effects of Casson parameter β, magnetic parameter M, stretching wedge parameter γ, Prandtl number Pr, radiation parameter N, Eckert number Ec, heat generation and absorption parameter ε suction/injection parameter S and Newtonian heating parameter δ are presented graphically with the following key points:
(a) Fluid velocity decreases as β and S increase when $\gamma > 1$ whereas increases when $\gamma < 1$.
(b) The dimensionless temperature decreases with the increase of M, β and S when $\gamma < 1$ and $\gamma > 1$.
(c) The thermal boundary layer is observed thicker with the increase of Ec and δ.
(d) The shear stress rate reduces with the growth of β while the effect of M is noted opposite.
(e) The local Nusselt number increases with the increase of N and β.
(f) The rate of heat transfer declines with the growth of Ec.

Acknowledgement

References

[1] Casson, N. 1959. A Flow Equation of Pigment Oil Suspensions of the Printing Ink Type. Mill CC. *Rheology of Disperse Systems*. Pergemon Press. 84-102.
[2] Eldabe, N. T. M. and Salwa, M. G. E. 1995. Heat Transfer of MHD Non-Newtonian Casson Fluid Flow between Two Rotating Cylinders. *Journal of Physical Society of Japan*. 64: 41-64.
[3] Dash, R. K., Mehta, K. N. and Jayaraman, G. 1996. Casson Fluid Flow in a Pipe Filled with a Homogeneous Porous Medium. *International Journal of Engineering Science*. 34: 1145-1156.
[4] Falkner, V. M. and Skan, S. W. 1931. Some Approximate Solutions of the Boundary-Layer for Flow Past a Stretching Boundary. *SIAM Journal of Applied Mathematics*. 49: 1350-1358.
[5] Ishak, A., Nazar, R. and Pop, I. 2007. Falkner-Skan Equation for Flow Past a Moving Wedge with Suction or Injection, *Journal of Appliled Mathematics and Computations*. 25: 67-83.
[6] Yacob, N. A., Ishak, A., Nazar, R. and Pop, I. 2011. Falkner-Skan Problem for a Static and Moving Wedge with Prescribed Surface Heat Flux in a Nanofluid. *International Communications in Heat and Mass Transfer*. 38: 149-153.
[7] Postelnicu, A. and Pop, I. 2011. Falkner-Skan Boundary Layer Flow of a Power-Law Fluid past a Stretching Wedge. *Appl. Math. Comput*. 217: 4359-4368.
[8] Mukhopadhyay, S., Mondal, I. C. and Chamkha, A. J. 2013. Casson Fluid Flow and Heat Transfer past a Symmetric Wedge. *Heat Transfer Research*. 42: 665-675.
[9] Mukhopadhyay, S. and Mandal, I. C. 2014. Boundary Layer Flow and Heat Transfer of a Casson Fluid past a Symmetric Porous Wedge with Surface Heat Flux. *Chinese Physics B*. 23: 044702.
[10] Yih, K. A. 1999. MHD Forced Convection Flow Adjacent to a Non-Isothermal Wedge, *International Communications in Heat and Mass Transfer*. 26: 819-827.
[11] Chamkha, A. J., Mujtaba, M., Quadri, A. and Issa, C. 2003. Thermal Radiation Effects nn MHD Forced Convection Flow Adjacent to a Non-Isothermal Wedge in the Presence of a Heat Source or Sink. *Heat and Mass Transfer* 39: 305-312.
[12] Su, X. L., Zheng, L., Zhang, X. and Zhang, J. 2012. MHD Mixed Convective Heat Transfer over a Permeable Stretching Wedge with Thermal Radiation and Ohmic Heating. *Chemical Engineering Science*. 78: 1-8.
[13] Prasad, K. V., Datti, P. S. and Vajravelu, K. 2013. MHD Mixed Convection Flow over a Permeable Non-Isothermal Wedge. *Journal of King Saud University-Science*. 25: 313-324.
[14] El-Dabe, N. T., Ghaly, A. Y. Rizkallah, R. R., Ewis, K. M. and Al-Bareda, A. S. 2015. Numerical Solution of MHD Boundary Layer Flow of Non-Newtonian Casson Fluid on a Moving Wedge with Heat and Mass Transfer and Induced Magnetic Field. *Journal of Applied Mathematics and Physics*. 3: 649-663.
[15] Hsiao, K. L. 2017. To Promote Radiation Electrical MHD Activation Energy Thermal Extrusion Manufacturing System Efficiency by using Carreau-Nanofluid with Parameters Control Method. *Energy*. 130: 486-499.
[16] Salem, A. M., El-Aziz, M. A. 2008. Effect of Hall Currents and Chemical Reaction on Hydromagnetic Flow of a Stretching Vertical Surface with Internal Heat Generation/Absorption. *Applied Mathematical Modelling*. 32: 1236-1254.
[17] Magyari, E., Chamkha, A. J. 2010. Combined Effect of Heat Generation or Absorption and First-order Chemical Reaction on Micropolar Fluid Flows Over a Uniformly Stretched Permeable Surface. *International Journal of Thermal Sciences*. 49: 1821-1828.
[18] Ahmad, R. and Khan, W. A. 2013. Effect of Viscous Dissipation and Internal Heat Generation/Absorption on

Heat Transfer Flow over a Moving Wedge with Convective Boundary Condition. *Heat Transfer Research.* 42: 589-602.

[19] Nandy, S. K., Mahapatra, T. R. 2013. Effects of Slip And Heat Generation/Absorption on MHD Stagnation Flow of Nanofluid Past a Stretching/Shrinking Surface with Convective Boundary Conditions. *International Journal of Heat and Mass Transfer.* 64: 1091-1100.

[20] Pal, D., Mandal, G. 2015. Mixed Convection-radiation on Stagnation-point Flow of Nanofluids over a Stretching/Shrinking Sheet in a Porous Medium with Heat Generation and Viscous Dissipation. *Journal of Petroleum Science and Engineering.* 126: 16-25.

[21] Hsiao, K.-L. 2016b. Stagnation Electrical MHD Nanofluid Mixed Convection with Slip Boundary on a Stretching Sheet. *Applied Thermal Engineering*. 98: 850-861.

[22] Hsiao, K.-L. 2016a. Combined Electrical MHD Heat Transfer Thermal Extrusion System Using Maxwell Fluid with Radiative and Viscous Dissipation Effects. *Applied Thermal Engineering*. 112: 1281-1288.

[23] Ferdows, M., Liu, D., 2017. Similarity Solutions on Mixed Convection Heat Transfer from a Horizontal Surface Saturated in a Porous Medium with Internal Heat Generation. *International Journal of Applied Mechanics and Engineering*. 22: 253-258.

[24] Cebeci, T. and Bradshaw, P. 1984. *Physical and Computational Aspects of Convective Heat Transfer*. Springer Verlag, New York.